2016 JMD CME Program

The Journal of Molecular Diagnostics, Vol. 18, No. 4, July 2016

ELSEVIER

the Journal of Molecular Diagnostics

jmd.amjpathol.org

A Rapid and Sensitive Next-Generation Sequencing Method to Detect *RB1* Mutations Improves Care for Retinoblastoma Patients and Their Families

Wenhui L. Li,[*†] Jonathan Buckley,[*†] Pedro A. Sanchez-Lara,[*†‡] Dennis T. Maglinte,[*] Lucy Viduetsky,[*] Tatiana V. Tatarinova,[‡§] Jennifer G. Aparicio,[¶] Jonathan W. Kim,[¶‖] Margaret Au,[*] Dejerianne Ostrow,[*] Thomas C. Lee,[¶‖] Maurice O'Gorman,[*†] Alexander Judkins,[*†] David Cobrinik,[¶‖**††‡‡] and Timothy J. Triche[*†]

From the Department of Pathology and Laboratory Medicine,[*] the Vision Center,[¶] the Division of Ophthalmology and Department of Surgery, and Saban Research Institute,[**] Children's Hospital Los Angeles, Los Angeles; the Departments of Pathology,[†] Pediatrics,[‡] Opthalmology,[‖] and Biochemistry & Molecular Biology,[††] USC Roski Eye Institute, and the Norris Comprehensive Cancer Center,[‡‡] USC Keck School of Medicine, and the Spatial Sciences Institute,[§] Dornsife College of Letters, Arts and Sciences, University of Southern California, Los Angeles, California

CME Accreditation Statement: This activity ("JMD 2016 CME Program in Molecular Diagnostics") has been planned and implemented in accordance with the Essential Areas and policies of the Accreditation Council for Continuing Medical Education (ACCME) through the joint providership of the American Society for Clinical Pathology (ASCP) and the American Society for Investigative Pathology (ASIP). ASCP is accredited by the ACCME to provide continuing medical education for physicians.

The ASCP designates this journal-based CME activity ("JMD 2016 CME Program in Molecular Diagnostics") for a maximum of 36 *AMA PRA Category 1 Credit(s)*™. Physicians should claim only credit commensurate with the extent of their participation in the activity.

CME Disclosures: The authors of this article and the planning committee members and staff have no relevant financial relationships with commercial interests to disclose.

Accepted for publication February 1, 2016.

Address correspondence to Wenhui L. Li, Ph.D., or Timothy J. Triche, M.D., Ph.D., Department of Pathology and Laboratory Medicine, Children's Hospital Los Angeles, 4650 Sunset Blvd, Mailstop 103, Los Angeles, CA 90027. E-mail: lauli@chla.usc.edu or ttriche@chla.usc.edu.

Retinoblastoma is a childhood eye malignancy that can lead to the loss of vision, eye(s), and sometimes life. The tumors are initiated by inactivating mutations in both alleles of the tumor-suppressor gene, *RB1*, or, rarely, by *MYCN* amplification. Timely identification of a germline *RB1* mutation in blood samples or either somatic *RB1* mutation or *MYCN* amplification in tumors is important for effective care and management of retinoblastoma patients and their families. However, current procedures to thoroughly test *RB1* mutations are complicated and lengthy. Herein, we report a next-generation sequencing–based method capable of detecting point mutations, small indels, and large deletions or duplications across the entire *RB1* gene and amplification of *MYCN* gene on a single platform. From DNA extraction to clinical interpretation requires only 3 days, enabling early molecular diagnosis of retinoblastoma and optimal treatment outcomes. This method can also detect low-level mosaic mutations in blood samples that can be missed by routine Sanger sequencing. In addition, it can differentiate between *RB1* mutation– and *MYCN* amplification–driven retinoblastomas. This rapid, comprehensive, and sensitive method for detecting *RB1* mutations and *MYCN* amplification can readily identify *RB1* mutation carriers and thus improve the management and genetic counseling for retinoblastoma patients and their families. *(J Mol Diagn 2016, 18: 480–493; http://dx.doi.org/10.1016/j.jmoldx.2016.02.006)*

Supported by the Department of Pathology and Laboratory Medicine, Children's Hospital Los Angeles, the Department of Defense (T.J.T.). The Larry and Celia Moh Foundation (D.C.), and an unrestricted departmental grant from Research to Prevent Blindness (J.W.K., T.C.L., and D.C.). Supported in part by The National Institute for General Medical Studies grant GM068968 (T.V.T.) and the Eunice Kennedy Shriver National Institute of Child Health and Human Development grant HD070996 (T.V.T.).

Disclosures: None declared.

http://dx.doi.org/10.1016/j.jmoldx.2016.02.006

Retinoblastoma is a malignant retinal tumor that occurs most often in the first 3 years of life.[1] It can occur either as a hereditary form or a nonhereditary form, with an overall incidence of approximately one in 15,000 to 20,000 live births.[2,3] Without proper management, retinoblastoma leads to metastatic disease and death, which occurs in 50% to 70% of affected children worldwide but in <5% of children in developed countries with advanced medical care.[4,5]

Retinoblastoma can present as a bilateral or unilateral disease. Nearly all bilateral retinoblastomas are caused by a heritable germline mutation in the *RB1* gene,[6–10] with the remainder caused by a mosaic *RB1* mutation or rarely by unknown etiology. Germline *RB1* mutations can also lead to nonocular malignancies in both childhood and adulthood; these tumors (notably osteosarcoma, the most common second malignancy) are generally more aggressive and less curable than retinoblastoma, highlighting the importance of identifying germline carriers.[11] Most unilateral retinoblastomas are nonhereditary and are caused by *RB1* somatic mutations during retinal development, although 10% to 15% of unilateral retinoblastoma patients carry germline mutations.[1,12] Determining whether mutations are germline or somatic is essential for establishing prognosis, implementing cancer screening regimens, and guiding genetic counseling of retinoblastoma patients and their families. Accordingly, rapid molecular diagnosis can facilitate patient management and improve treatment outcomes by identifying patients and family members who are at risk for second malignancies.

Identifying disease-causing *RB1* mutations can be a lengthy process, often requiring weeks or months to do thorough analyses.[13] *RB1* is a large gene containing approximately 183,000 bp with 27 exons, and analyses have historically been limited to the coding exons and flanking intronic sequences. In retinoblastoma, 11 recurrent premature termination codon mutations comprise approximately 22% of all *RB1* mutations,[14] with the remainder composed of various types of mutations scattered throughout the gene.[15–18] Clinical laboratories use a variety of methods to ensure comprehensive *RB1* testing, including Sanger sequencing to identify point mutations and small insertions and deletions (indels) in exons and in exon-intron splicing junctions. Large deletions and duplications in the *RB1* gene can be detected by an alternate technology, such as multiplex ligation-dependent probe amplification (MLPA) or quantitative multiplex PCR.[13] However, mutations that occur deep within introns can also affect splicing, resulting in intron retention, exon skipping, and frame shifts, all of which result in nonfunctional *RB1* protein[19–23] yet are not detected by current DNA testing. Data have shown that using RT-PCR to detect intron mutations outside of canonical splice sites in the *RB1* gene could improve overall sensitivity from 89% to 92%; however, false-negative results are always a concern because incorrectly spliced RNAs can be far less stable than wild-type RNA.[20]

Another challenge in *RB1* mutation screening is distinguishing low-level mosaic mutations versus somatic mutations. Because the heritable form of retinoblastoma is an autosomal dominant condition, the first affected family member can have either a *de novo* germline mutation (likely resulting from a new mutation in a parent's gametes) or a mosaic mutation that arose during early embryogenesis. In approximately 10% of families, the initial *RB1* mutation is mosaic, either in the proband or in one of the proband's parents.[24] The ability to identify *RB1* mosaicism is critical for genetic counseling of probands because mosaicism confers risk for retinoblastoma in the other eye, second cancers, and passing the mutation to progeny. To detect low-level mosaic mutations in blood samples, mutations are often first identified in tumor samples, followed by allele-specific PCR confirmation in DNA from blood. However, this strategy cannot be used for patients whose tumors are treated focally without enucleation, because no reference tumor mutation information will be available. In addition, low-level mosaicism could exist in a phenotypically normal parent. To identify such mutation in the parent is essential for accurate genetic counseling. Recently, a next-generation sequencing (NGS)–based method was described to detect low-level mosaic *RB1* mutations, but only in *RB1* exons.[25]

An additional challenge is to define the molecular etiology of retinoblastoma when no *RB1* mutations are detected. Rushlow et al[26] documented that 2% to 3% of childhood retinal tumors do not have an *RB1* mutation that can be identified using current approaches. Approximately 50% of these tumors had *MYCN* gene amplification with several distinct tumor properties.[26] Retinoblastoma with *MYCN* amplification has an aggressive phenotype and resembles *MYCN* amplified neuroblastoma histologically as well as etiologically. Because *MYCN* amplification in combination with wild-type *RB1* has been observed only in nonhereditary retinoblastoma, in cases where no *RB1* mutation can be found, *MYCN* amplification status can be tested to differentiate between *RB1* mutation and *MYCN* amplification–driven retinoblastomas.

Because of clinically relevant technological advances combined with the plummeting cost of NGS technology, it is possible to perform massively parallel sequencing of the entire *RB1* and *MYCN* genes in a timely and cost-efficient manner. Herein, we describe an NGS-based method that sequences the entire *RB1* gene, including promoter, untranslated regions, exons, and introns, with an average coverage >500×, and simultaneously determines *MYCN* copy number. The ability of this method to detect single-nucleotide substitutions, small indels, and large deletions/duplications across the *RB1* gene and the amplification of *MYCN* gene was evaluated. In addition, we investigated the possibility of detecting mosaic mutations in the *RB1* gene directly from blood samples using this method.

Materials and Methods

Retinoblastoma Samples and Reference Samples

Deidentified samples from patients with retinoblastoma were obtained from the Children Hospital Los Angeles (CHLA) genomic laboratory and the CHLA Retinoblastoma Tissue Bank under CHLA Institutional Review Board protocol CCI#09-00322. DNA was extracted from flash-frozen retinoblastoma tumor tissues or from EDTA blood samples. A total of 30 blood samples, 11 tumor samples, and one reference sample (NA12878) from 1000 Genome Project (*http://www.1000genomes.org*, last accessed April 2, 2014) was used for the analysis.

Haloplex *RB1* Target Capture and Enrichment

Haloplex target capture probes were designed using SureDesign software version 1.0 (Agilent Technologies, Santa Clara, CA). The target regions include the entire *RB1* gene, as well as *GAPDH* exons and *MYCN* exons (Supplemental Table S1). Haloplex DNA libraries were built from extracted genomic DNA using Haloplex Target Enrichment kit (Agilent Technologies), according to the manufacturer's protocols. Because sufficient sequence data could be generated when pooling two libraries per Ion Torrent 318 version 2 chip, an equimolar pool of two barcoded Haloplex libraries was generated for pairs of samples. Emulsion PCR using the OneTouch2 system (Life Technologies, Carlsbad, CA) was performed after library construction.

NGS and Data Analysis

The amplified libraries were sequenced on the Ion Personal Genome Machine (Life Technologies). Signal processing, base calling, and alignment were performed using the default settings of Torrent Suite 4.0 (Life Technologies). All reads were then aligned to the entire reference genome, human hg19, using alignment plugin 4.0-r70791. Variant calling was performed via Torrent Suite Variant Caller plugin v4.0-r73742 (Life Technologies). Variant calling was restricted to the regions covered by the RB1 HaloPlex assay. Variant calling files from Torrent Suite were uploaded to BENCHlab NGS and categorized as likely benign, benign, variant of unknown significance, and likely pathogenic. *RB1* mutations that were classified as likely pathogenic were confirmed by manual curation, then their classifications were changed to pathogenic. The procedure from the beginning of DNA extraction to clinical interpretation can be completed in 3 days.

Confirmation of Mutations in *RB1* by Sanger Sequencing

Germline mutations identified by the RB1 NGS method were confirmed by Sanger sequencing. PCR forward and reverse primers were designed using online software tool Primer3 version 0.4.0 (*http://bioinfo.ut.ee/primer3-0.4.0/primer3*, last accessed April 2, 2014) (Table 1). The target regions were PCR amplified and cycle sequenced using the BigDye Direct Cycle Sequencing kit (Life Technologies), according to the manufacturer's instructions. The sequencing product was separated on an ABI 3730 genetic analyzer. Sanger sequencing data were analyzed by Mutation Surveyor (V4.0.9). Mosaic mutations were also confirmed by the Sanger sequencing method. Extreme low levels of mosaic mutations cannot be confirmed by Sanger sequencing method; however, allele-specific PCR can be used for confirmation, as described.[14]

RB1 and *MYCN* Deletion or Duplication Analysis

Coverage value at each base in the *RB1* and *GAPDH* genes was adjusted to reduce systematic variations in coverage across the gene (patterns consistent across samples, reflecting differential sequencing efficiency because of local factors, such as local GC content) and overall sequence efficiency of the run. If c_i is the coverage at genomic position i, the adjusted coverage a_i is

$$f\frac{c_i}{n_i} \quad (1)$$

where n_i is the average coverage at the position i from a reference set of normal (no copy number changes) samples, and the relative run efficiency, f, is twice the ratio of the mean coverage over *GAPDH* (used as a reference gene) to the mean *GAPDH* coverage in the reference set. The a_i values, plotted across the *RB1* gene, are expected to be distributed around 2 for diploid cells. The overall (average) *RB1* copy number is as follows:

$$CV = f\frac{R}{532}, \quad (2)$$

where R is the mean coverage of the sample over *RB1*, and 532 is equal to the mean coverage over *RB1* in the reference set. The *MYCN* copy number was determined, as above, for *RB1*.

Promoter Analysis

The upstream promoter sequence of *RB1* gene (corresponding coding DNA sequence positions 48303912 to 48480070) on chromosome 13 (GRCh38 Primary Assembly) was obtained from the National Center for Biotechnology Information. The position of the transcription start site (TSS) at the position of −161 upstream from ATG was validated using TSSer[27] and NPEST[28] algorithms. CHLA normal samples ($n = 15$) and 1000 Genomes samples ($n = 1092$) were used for the promoter analysis.

Mosaic Mutation Analysis

To establish a mosaic-calling algorithm, we performed two sets of admixture studies in which DNA from two

Table 1 RB1 Sanger Sequencing Primers

Exon	Forward primer	Reverse primer
1	5′-TGTAAAACGACGGCCAGTGGTTTTTCTC-AGGGGACGTT-3′	5′-CAGGAAACAGCTATGACCAACCCAGAATC-CTGTCACCA-3′
2	5′-TGTAAAACGACGGCCAGTTGTTATGTGC-AAACTATTGAAACAA-3′	5′-CAGGAAACAGCTATGACCGGTAAATTTCCTC-TGGGTAATGG-3′
3	5′-TGTAAAACGACGGCCAGTTGCCATCAGA-AGGATGTGTT-3′	5′-CAGGAAACAGCTATGACCTTGGTCCAAGTTC-TTTTTGTTTT-3′
4	5′-TGTAAAACGACGGCCAGTTTTGATGTAGA-GCTGATAATCTTTTG-3′	5′-CAGGAAACAGCTATGACCAATTCCCAGAATCT-AATTGTGAAC-3′
5	5′-TGTAAAACGACGGCCAGTTTGGGAAAATC-TACTTGAACTTTGT-3′	5′-CAGGAAACAGCTATGACCGCCTGCTATAATTCG-ATCAAACT-3′
6	5′-TGTAAAACGACGGCCAGTAAATTATGCAAT-TAAAATGGACTGC-3′	5′-CAGGAAACAGCTATGACCTTTAGTCCAAAGGAA-TGCCAAT-3′
7	5′-TGTAAAACGACGGCCAGTCTACCCTGCGAT-TTTCTCTCA-3′	5′-CAGGAAACAGCTATGACCGAGAAAGTAAAAGGG-GCATAAAT-3′
8	5′-TGTAAAACGACGGCCAGTGAATGTTACCAA-GATTATTTTTGACC-3′	5′-CAGGAAACAGCTATGACCTGCTACTGCAAAAGA-GTTAGCAC-3′
9	5′-TGTAAAACGACGGCCAGTTGGGGGATTGAC-ACCTCT-3′	5′-CAGGAAACAGCTATGACCATCCTCCCTCCACAGT-CTCA-3′
10	5′-TGTAAAACGACGGCCAGTATCTGTGCCTCT-GTGTGCTG-3′	5′-CAGGAAACAGCTATGACCTCAATCAAATATACCA-TGTGCAA-3′
11	5′-TGTAAAACGACGGCCAGT GCAGCAGCTGG-GTCATCTAT-3′	5′-CAGGAAACAGCTATGACCTCTGAAACACTATAAA-GCCATGAA-3′
12	5′-TGTAAAACGACGGCCAGTAGACAAGTGGGA-GGCAGTGT-3′	5′-CAGGAAACAGCTATGACCGCAAGAAAAGATTATGG-ATAACTACA-3′
13	5′-TGTAAAACGACGGCCAGTTGGAAGTGTTTC-CACATTTTT-3′	5′-CAGGAAACAGCTATGACCCACAGGCAGCAGGGAT-ATAG-3′
14	5′-TGTAAAACGACGGCCAGTGGGCAAAACAG-TGAGACTCC-3′	5′-CAGGAAACAGCTATGACCCCAAAGTGCTGGG-ATTGC-3′
15	5′-TGTAAAACGACGGCCAGTATGCTGACACAA-ATAAGGTTT-3′	5′-CAGGAAACAGCTATGACCATTATAAAATACTTACT-TCTATAAAAA-3′
16	5′-TGTAAAACGACGGCCAGTTGCTGACACAAA-TAAGGTTTCA-3′	5′-CAGGAAACAGCTATGACCGCATTCCTTCTCCTT-AACCTCA-3′
17	5′-TGTAAAACGACGGCCAGTAAAATTGGAAGG-CTATTTCC-3′	5′-CAGGAAACAGCTATGACCATAATTTGTTAGCCAT-ATGCAC-3′
18	5′-TGTAAAACGACGGCCAGTCCACTGTCAATT-GTGCCTAAAA-3′	5′-CAGGAAACAGCTATGACCTTGCAGTTTGAATGG-TCAACA-3′
19	5′-TGTAAAACGACGGCCAGTCCAACTTGAAAT-GAAGACTTTTCC-3′	5′-CAGGAAACAGCTATGACCCATGATTTGAACCCA-GTCAGC-3′
20	5′-TGTAAAACGACGGCCAGTAATTCAAAATGA-ACAGTAAAAATGAC-3′	5′-CAGGAAACAGCTATGACCCAACACTTTGGGAGGC-CTTA-3′
21	5′-TGTAAAACGACGGCCAGTTGAGGCTAAAAG-AAAGAAAATGG-3′	5′-CAGGAAACAGCTATGACCTGAATAAATGAGATCAAA-TGAATTACC-3′
22 and 23	5′-TGTAAAACGACGGCCAGTAATATGTGCTTCT-TACCAGTCAAA-3′	5′-CAGGAAACAGCTATGACCGGATCAAAATAATCCC-CCTCTC-3′
24	5′-TGTAAAACGACGGCCAGTTGTCAGTGGTTC-TAGGGTAGAGG-3′	5′-CAGGAAACAGCTATGACCGCAATATGCCTGGATG-AGGT-3′
25	5′-TGTAAAACGACGGCCAGTTGCCTGATTTTTT-GACACACC-3′	5′-CAGGAAACAGCTATGACCCTCTGGATTCCCCAG-ATGAC-3′
26	5′-TGTAAAACGACGGCCAGTCACATGAAATGT-TTTGCATTTTT-3′	5′-CAGGAAACAGCTATGACCCAAACCTGCCAACTG-AAGAA-3′
27	5′-TGTAAAACGACGGCCAGTCGCCATCAGTTT-GACATGAG-3′	5′-CAGGAAACAGCTATGACCAGTGTCCACCAAGGTCC-TGA-3′

samples was combined in varying proportion. The first experiment was set up using two samples with sample ratios as 100:0, 95:5, 90:10, 75:25, 50:50, 25:75, 10:90, 5:95, and 0:100; the second experiment was set up using two different samples (from the first experiment) with sample ratios as 100:0, 85:15, 50:50, 25:75, 20:80, 15:85, 10:90, and 0:100. Single-nucleotide polymorphisms (SNPs) that were heterozygous in one sample but

homozygous in the other were identified as pseudomosaic markers, to be used in developing and testing the algorithm.

MLPA Copy Number Analysis

SALSA MLPA KIT P047-C1 RB1 and related reagents are designed and manufactured by MRC-Holland (Amsterdam, the Netherlands). They were used to detect exon deletions or duplications in *RB1*. The MLPA assay was performed according to the manufacturer's protocol, and MLPA data were analyzed by GeneMarker software version 2.6.0 (Softgenetics, State College, PA).

Real-Time Quantitative PCR Method to Quantify Copy Number of the *MYCN* Gene

A TaqMan Copy Number MYCN Assay Hs02029019 was run simultaneously with a TaqMan Copy Number Reference Assay (Life Technologies) in a duplex real-time PCR. Hs02029019 detects the target *MYCN* gene, and the Reference Assay detects the human RNase P H1 RNA gene that is known to exist in two copies in a diploid genome. The number of copies of the *MYCN* gene in each test sample was determined by relative quantitation using the comparative CT ($\Delta\Delta C_T$) method.

Results

Coverage of the *RB1* Gene

We analyzed separately the coverage of *RB1* exons, exons plus 2 bp splice junctions, the *RB1* promoter, and the entire *RB1* gene including the promoter and all exons and introns in eight blood samples from retinoblastoma patients (Figure 1A). The average coverage on each *RB1* exon varied; however, it was reproducible and ranged from 80× on exon 15 to 2300× on exon 27. The average coverage was 693× for *RB1* exons plus 2 bp splice junctions, and 572× for the entire *RB1* gene. The percentage of coverage as a function of the coverage depth was also evaluated (Figure 1B). The *RB1* exons were reproducibly covered 100% above 10×, 99.99% above 20×, and 99.97% above 30×, respectively. The promoter and the entire *RB1* gene was consistently covered above 94% at 1×, 92% at 10×, and 89% at 30×, respectively. The regions in the *RB1* gene with zero coverage were situated within the highly repetitive sequences in *RB1* introns, where it was not possible to design unique probes; this represents a total of 10,963 bp of intronic sequence (Supplemental Table S2). To determine whether the RB1 NGS test would miss any previously reported *RB1* mutations, we performed the coverage analysis at all positions where variants have been reported in the Human Genome Mutation Database (HGMD; registration required; *http://www.hgmd.org*, last accessed April 2, 2014). There are 165 missense/nonsense mutations, 151 splicing mutations, 10 regulatory promoter mutations, 216 small deletions, and 78 small insertions in HGMD (version 2013.3). This *RB1* NGS test had minimum coverage of 20× for all these positions, with most covered well above 30× in all eight retinoblastoma blood samples examined (data not shown). The HGMD included 156 *RB1* intronic mutations, 68 of them outside the 2 bp exon/intron splice junctions commonly assessed. Ten deep intronic mutations, which are >20 bp distant from splice junctions, were proved to be pathogenic[19–23] and covered above 20× by the *RB1* NGS test. Our test is the first test that can routinely screen these pathogenic, deep intronic mutations in every patient. Dependent on the recurrent frequency of these deep intronic mutations, detection of such mutations might just slightly improve the overall mutation detection rate, but will be critically important for the rare families carrying such mutations. Although our test could not determine the pathogenicity of novel intronic mutations, the detection of such mutations in patients with no identified pathogenic mutation could encourage a decision to define its significance by *RB1* RNA analysis in the research setting, whereas a lack of novel deep intron SNVs would argue against pursuing the RNA analysis.

Detection of Genetic Variants in *RB1*

To evaluate the test's ability to detect *RB1* genetic variants, we used two approaches recommended by the American College of Medical Genetics.[29] First, our method was tested using one Hapmap sample, NA12878. NA12878's genotype data were downloaded from Illumina's Platinum Genomes website (*http://www.illumina.com/platinumgenomes*, last accessed April 2, 2014); additional variant calling files are also available for both parents of the individual, providing the means to validate all called variants in the sample. The genotype of NA12878 was confirmed by comparing it with the genotypes of the parents. *De novo* variants and genotype calls not made in both parents were excluded. The genotypes were additionally filtered for those bases in the design bed file for the RB1 test, regions covered by a minimum read depth in all samples of the intraday and interday samples, respectively, whose quality filter was PASS and did not lie in or immediately precede a homopolymer greater or equal to seven bases. These filtered data sets became known as the Confirmed Illumina Platinum (CIP) data sets. NA12878 was used to assess the overall performance of the RB1 NGS test to detect diverse genetic variations across the entire *RB1* gene. Although all of the *RB1* variations observed in NA12878 are not pathogenic mutations, they can help assess the analytical performance of our method, knowing that the clinical significance of the variant has little bearing on its detectability.

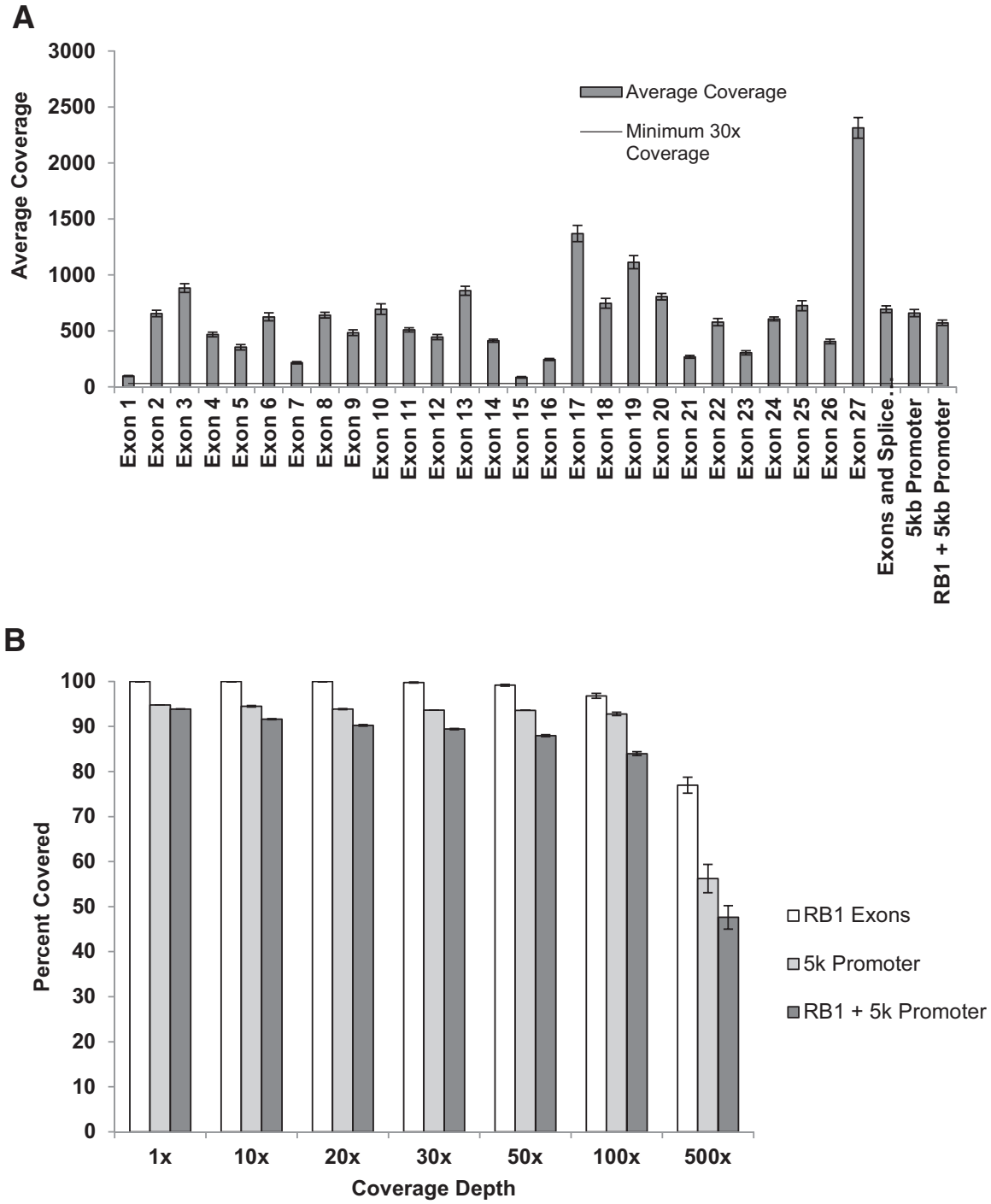

Figure 1 Coverage analysis of the RB1 next-generation sequencing test. **A:** The average coverage of each exon of *RB1* gene, exons plus 2 bp splice junctions, the *RB1* promoter, and the entire *RB1* gene was plotted (from eight retinoblastoma blood samples). The line represents the coverage depth of 30×. **B:** Percentage of *RB1* coverage on exons, the *RB1* promoter, and the entire *RB1* gene was plotted versus the coverage depth. The white, gray, and black bars represent the percentage of coverage on *RB1* exons, the *RB1* promoter, and the entire *RB1* gene, respectively.

The genotype calls generated from the public data set for NA12878's *RB1* gene were compared with the genotype calls generated through our RB1 NGS test. The total number of loci in *RB1*, after quality filtering, available for comparison was 156,603 bp. The genotypes at each locus were compared (RB1 NGS test versus Illumina's platinum genome data) to determine the number of false-positive variant calls (variants called with the RB1 NGS test not found in Illumina's data) and false-negative calls (in Illumina's data but not the RB1 NGS test variant calling file). We limited our comparison only to SNVs. To calculate sensitivity, variants identified by the RB1 NGS test were

Table 2 Concordance between CHLA RB1 NGS Test Result and Validated Illumina Data Set

CHLA RB1 NGS (Ion Torrent)	Variants (Illumina)	Wild type (Illumina)
Variants	121	2
Wild type	0	156,480

CHLA, Children Hospital Los Angeles; NGS, next-generation sequencing.

compared with the set of true positives. True positives were considered to be those bases in the CIP data set that were identified as heterozygous or homozygous variants versus the reference genome, hg19/National Center for Biotechnology Information 37. SNVs and insertions/deletions (indels) were considered separately. Concordance was measured as the variant calls by our RB1 NGS test that matched the variant calls in the CIP data set. To calculate specificity, wild-type calls identified by the RB1 NGS test were compared with the set of true negatives. True negatives were considered to be those bases in the CIP data sets that were identified as homozygous wild-type for the reference genome. Concordance was measured as the wild-type calls from RB1 NGS test that matched the reference genome and the wild-type calls in the CIP data set. The RB1 NGS test detected all Illumina-validated variants in NA12878, which yields a 100% sensitivity to detect SNVs. Two additional variant calls of 156,482 reference calls were detected by the RB1 NGS test and found to be false positive by Sanger sequencing, which gives a specificity of 99.99% (Table 2). Because the Ion Torrent sequencing platform gives false indel calls around

Table 3 RB1 NGS Test on Retinoblastoma Blood Samples

Sample ID	Laterality	Family history	Result from certified laboratory	RB1 NGS test result	Concordance
1	Unilateral	Isolated	Normal*†‡	Normal	Yes
2	Unilateral	Isolated	Normal*†‡	Normal	Yes
3	Bilateral	Isolated	c.2119delT*	c.2119delT	Yes
4	Unilateral	Isolated	Normal*†‡	Normal	Yes
5	Bilateral	Familial	del P->17†§	del P->17§	Yes
6	Unilateral	Isolated	Normal*†‡	Normal	Yes
7	Bilateral	Isolated	g.45867G>C (splice)*	c.607+1G>C (splice)	Yes
8	Bilateral	Isolated	c.2468delC*	c.2468delC	Yes
9	Bilateral	Isolated	c.508G>T (p.Glu170Stop)*	c.508G>T (p.Glu170Stop)	Yes
10	Unilateral	Isolated	Normal*†‡	Normal	Yes
11	Bilateral	Isolated	g.76933_76948del16*†	g.76933_76948del16	Yes
12	Bilateral	Isolated	c.763 C>T (p.Arg255Stop)*	c.763C>T (p.Arg255Stop)	Yes
13	Bilateral	Mother affected	c.1693_1694dupTC*†	c.1693_1694dupTC	Yes
14	Bilateral	Isolated	c.1306C>T (Gln436Stop)*	c.1306C>T (Gln436Stop)	Yes
15	Unilateral	Isolated	Normal*†‡	Normal	Yes
16	Unilateral	Isolated	Normal*†‡	Normal	Yes
17	Bilateral	Isolated	c1975_1981delTATCTCC*	c.1975_1981delTATCTCC	Yes
18	Bilateral	Isolated	c.1549delA*†	c.1549delA	Yes
19	Bilateral	Isolated	c.1390-2A>G*†	c.1390-2A>G	Yes
20	Bilateral	Isolated	Mosaic c.940-2A>T*†‡	Mosaic c.940-2A>T	Yes
21	Unaffected	Child affected	Mosaic c.508G>T*†‡ (p.Glu170Stop)	Mosaic c.508G>T (p.Glu170Stop)	Yes
22	Unaffected	Child affected	Normal*†‡	Normal	Yes
23	Unaffected	Child affected	VOUS (c.1876G>A, c.1966C>T, c.1815-5T>C)*	VOUS (c.1876G>A, c.1966C>T, c.1815-5T>C)	Yes
24	Unilateral	Child affected	c.1693_1694dupTC*†	c.1693_1694dupTC	Yes
25	Bilateral	Isolated	del P->27†	del P->27	Yes
26	Bilateral	Child affected	g.45867G>C*†	c.607+1G>C (splice)	Yes
27	Bilateral	NA	NA	c.1021A>T (K341Stop)	
28	Bilateral (one eye enucleation)	NA	NA	c.763C>T (p.Arg255Stop)	
29	Bilateral	NA	del P->27†¶	del P->27¶	Yes
30	Bilateral	NA	del P->27†¶	del P->27¶	Yes

*Sanger sequencing.
†Quantitative multiplex PCR.
‡Allele-specific PCR.
§del P->17, deletion of *RB1* gene from promoter to exon 17.
¶del P->27, deletion of *RB1* gene from promoter to exon 27.
NA, not available; NGS, next-generation sequencing.

Table 4 RB1 NGS Test on Retinoblastoma Tumor Samples

		RB1 result from another laboratory		RB1 NGS test result		
Sample	Laterality	Tumor allele 1	Tumor allele 2	Tumor allele 1	Tumor allele 2	Concordance
31	Unilateral	c.1363C>T (p.R455Stop)*	c.1363C>T (p.R455Stop)*	c.1363C>T (p.R455Stop)	c.1363C>T (p.R455Stop)	Yes
32	Unilateral	del P->27†	del P-27†	del P->27	del P-27	Yes
33	Unilateral	c.1399C>T (p.R467Stop)*	c.1399C>T (p.R467Stop)*	c.1399C>T (p.R467Stop)	c.1399C>T (p.R467Stop)	Yes
34	Bilateral	c751C>T (p.Arg251Stop)*	c1654C>T (p.Arg552Stop)*	c751C>T (p.Arg251Stop)	c1654C>T (p.Arg552Stop)	Yes
35	Unilateral	c.1030C>T (p.Gln344Stop)*	c.1030C>T (p.Gln344Stop)*	c.1030C>T (p.Gln344Stop)	c.1030C>T (p.Gln344Stop)	Yes
36	Unilateral	c.751C>T (p.Arg251Stop)*	c.2359C>T (p.Arg787Stop)*	c.751C>T (p.Arg251Stop)	c.2359C>T (p.Arg787Stop)	Yes
37	Unilateral	IVS3-2A>G (c.381-2A>G)*†	c.958C>T (p.Arg320Stop)*†	IVS3-2A>G (c.381-2A>G)	c.958C>T (p.Arg320Stop)	Yes
38	Unilateral	del exon 3->27†; dup Pro-exon 2†	del exon 3->27†; dup Pro-exon 2†	del exon 3->27; dup Pro-exon 2	del exon 3->27; dup Pro-exon 2	Yes
39	Unilateral	c. 409 G>T (p.Glu137Stop)*	c. 409 G>T (p.Glu137Stop)*	c. 409 G>T (p.Glu137Stop)	c. 409 G>T (p.Glu137Stop)	Yes
40	Unilateral	c.1735 C>T (p.Arg579Stop)*	del P->27†	c.1735 C>T (p.Arg579Stop)	del P->27	Yes
41	Unilateral	c.2174dupT*†	c. 769 C>T (p.Gln257Stop)*	c.2174dupT	c. 769 C>T (p.Gln257Stop)	Yes

*Sanger sequencing.
†Quantitative multiplex PCR.
NGS, next-generation sequencing.

homopolymer regions, all suspected pathogenic indel calls were reviewed by checking aligned sequencing data and sequencing quality controls and were confirmed by Sanger sequencing before the report was generated.

The second approach was to compare blinded sequencing results of our RB1 NGS test with the results obtained from 30 blood samples and 11 tumor samples tested at an independent retinoblastoma testing laboratory. This independent clinical laboratory uses quantitative multiplex PCR to measure copy number variations in the *RB1* gene, Sanger sequencing analysis to detect point mutations or indels, and allele-specific PCR to detect low levels of 11 recurrent *RB1* mosaic mutations. The results from our RB1 NGS test for blood and tumor samples matched 100% with results generated using non-NGS methods from a College of American Pathologists/Clinical Laboratory Improvement Amendment–certified retinoblastoma testing laboratory (Tables 3 and 4). Nonsense, splicing, and frameshift mutations were frequently observed in the retinoblastoma blood samples we tested, which is consistent with published data.[15–17] No promoter or in-frame indel mutations were found in these tested samples, probably because of the low frequency of such mutations.[15,17] In the retinoblastoma tumor specimens, large deletion and duplication events were frequently observed. Notably, we observed homozygous pathogenic point mutations of *RB1* in 4 of 11 retinoblastoma tumors. The result was confirmed by MLPA to rule out hemizygosity of the *RB1* locus.

Detection of Large Deletions or Duplications in *RB1*

Large deletions or duplications in *RB1* represent 16% of pathogenic *RB1* mutations found in retinoblastoma patients.[1] Currently, detecting such mutations requires a method independent from Sanger sequencing, such as real-time quantitative PCR or MLPA. NGS technology and deep sequencing coverage may be used to detect large deletions or duplications.[30] Herein, we sequenced the entire *RB1* gene from which all of the sequencing reads were used to help accurately determine copy number variations within the *RB1* gene. Because the size of *RB1* introns is much longer than that of exons (Figure 2A), being able to evaluate copy number changes of introns as well as exons significantly improves the confidence of calling a large deletion or duplication in the *RB1* gene. Sequencing reads of *RB1* were normalized first using sequencing reads from *GAPDH* (Supplemental Figure S1), then compared with the pool of reference samples. The copy number of RB1 was determined by Genetrix software version 3.74 (Epicenter Software, Pasadena, CA). We tested various retinoblastoma tumor samples with normal *RB1* copy number as well as those harboring large deletions or duplications (Figure 2). The RB1 NGS test detected a heterozygous whole gene deletion (Figure 2D) in one tumor sample, and homozygous partial gene deletion and partial gene multiplication (Figure 2D) in another tumor sample. The results were concordant with reports from another independent College

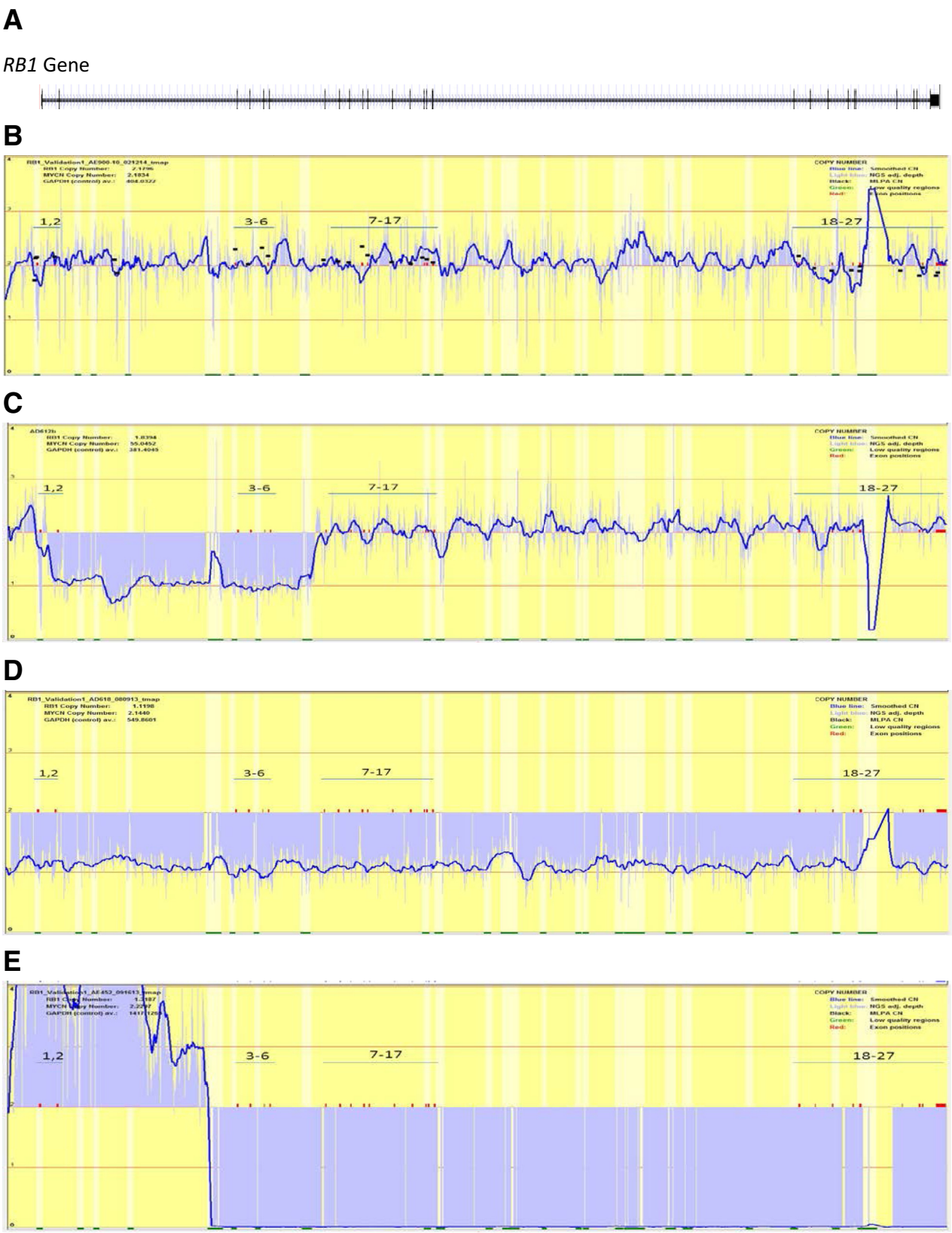

Figure 2 Copy number analysis of retinoblastoma samples. **A:** The entire *RB1* gene, with vertical lines representing *RB1* exons and introns between, is shown on the top. **B**—**E:** The light blue traces represent adjusted depth at all *RB1* positions; the **dark blue line** represents the smoothed copy number (CN); and *RB1* exons are labeled as four exon islands: exons 1 to 2, 3 to 6, 7 to 17, and 18 to 27. **B:** No copy number change in a retinoblastoma tumor sample. **C:** Heterozygous internal deletion of exons 2 to 6 in a retinoblastoma cell line Y79. **D:** Heterozygous deletion of entire *RB1* gene in a retinoblastoma tumor sample. **E:** Homozygous deletion of exon 3 to 27 and multiplication of promoter-exon 2 of *RB1* gene in a retinoblastoma tumor sample.

of American Pathologists/Clinical Laboratory Improvement Amendment–certified laboratory that uses the real-time quantitative PCR method, as well as with MLPA assay results (Supplemental Figure S2). The heterozygous internal deletion of exons 2 to 6, spanning approximately 52 kb in the retinoblastoma cell line Y79, was easily detected by the RB1 NGS test (Figure 2C). The method reported herein can reliably detect germline copy number changes, but not mosaic copy number changes (data not shown).

Systematic Detection of Mosaic *RB1* Mutations

Deep sequencing of *RB1* provides a method for direct detection of low-level mosaic mutations in blood samples. Recognition of mosaicism requires initial identification of the variant (at low frequency) with subsequent determination that relative mutant and wild-type allele frequencies depart significantly from the expected 1:1 ratio. We established a mosaic-calling algorithm in Genetrix that uses the Ion Torrent somatic variant calling pipeline and its quality thresholds for input data. We determined that detection of lower-level mosaicism in regions susceptible to read errors (eg, in the vicinity of homopolymers) or with marginal coverage was problematic. However, the emphasis in developing a mosaic variant algorithm is primarily to protect against false positives. The serial dilution of two samples' DNA generated nine different admixtures with various proportions of each sample ranging from 0% to 100%. These admixtures provide informative SNPs with nominal minor allele frequencies ranging from 2.5% to 47.5% (corresponding to percentage representation of the variant-containing sample from 5% to 95%). We analyzed 15 pseudomosaic variants (nine heterozygous in one sample, six in the other) in admixture samples (Figure 3A). For each admixture, at each informative SNP location, the quality score assigned to each variant by the Ion Torrent variant caller (which is strongly influenced by deviations in allele frequency from 1:1) was used in Genetrix to filter out unreliable calls. In Genetrix, a sliding scale was established for the mosaic mutation calling on the basis of the measured mosaicism frequency (MF). For MF <10, the quality score cutoff was set to 10; for MF 11 to 25, the cutoff was 40; for MF 26 to 50, the cutoff was 100; for MF 51 to 75, the cutoff was 200; and for MF >76, the cutoff was 400 (Figure 3A). In developing the algorithm, we also considered incorporation of read depth information as a separate quality control parameter, but we observed that no extra value was added because the variant call quality score is already dependent on read depth, so we elected to base our cutoffs on quality score alone.

With the above quality score cutoffs, the 15 SNPs were not called in either of the two samples with 0% admixture. However, from 5% to 75%, all variant quality scores exceeded the thresholds and the variant was called. At 90%, all 15 SNP variants were again called. However, one SNP had a measured mosaicism $>90\%$ and was thus called as a nonmosaic variant. At 95%, 4 of 15 SNPs were called nonmosaic. Thus, of 70 variants present at nominal frequencies corresponding to admixtures in the range of 5% to 90%, all were detected and all but one were correctly recognized as mosaic. At an admixture rate of 95%, all were called but the presence of mosaicism was missed in 4 of 15 SNPs.

Evaluation was repeated for the second experiment in which a total of eight different admixtures were generated with various proportions of each sample ranging from 0% to 100%. In this experiment, 54 of 55 mosaic variants from samples with admixture proportions in the range of 5% to 90% were correctly called mosaics; the one exception was a sample with 85% representation, which was called nonmosaic. The algorithm identified 4 of 10 nonmosaic variants (with no admixture) as mosaic, but in each instance, the mosaicism fraction was measured to be $>85\%$.

To establish an upper limit for calling mosaicism, the distribution of the ratio of the variant read count to total count was examined in 95 true heterozygous SNPs in the *RB1* gene. The mean of this ratio was 48.72%, with an SD of 3.21; we set the upper limit for mosaicism to correspond to three SDs lower than the mean (39.1% variant allele, equivalent to a cellular mosaicism estimate of 78.2%) to minimize false positives arising because of stochastic variation in allele counts at a heterozygous (nonmosaic) locus. Potential false positives at low variant allele frequency are more likely to result from read or alignment errors. To minimize these, we manually inspect the read alignments, and associated statistics related to variant/wild-type differences in strand, position in read, or base quality score. For the lower limit of calling mosaicism, the somatic variant caller was effective in identifying pseudomosaic variants down to 5% (ie, 5% of cells containing the variant and 95% wild-type). False positives were effectively eliminated using an empirical quality score filter, with threshold levels adjusted according to the measured mosaicism frequency. Variant-carrying mosaic cells with a measured percentage $<5\%$ were reported as nonmosaic wild-type. Taken together, we set the variant-calling thresholds as following: variant-carrying mosaic cells with a measured percentage $<5\%$ were flagged as nonmosaic wild-type; those $>78.2\%$ were flagged as nonmosaic heterozygous. A flagged mosaic variant that is suspected to be pathogenic is confirmed by Sanger sequencing or allele-specific PCR before clinical reporting.

The data presented in Figure 3 reflect performance for selected polymorphic sites and cannot be extended to problematic regions with low coverage and/or high read errors where lower-quality scores will result in reduced sensitivity for detecting mosaic mutations. Mosaic mutations residing in such problematic regions could be missed by our mosaic-calling algorithm.

Using this algorithm, we detected mosaic mutations in two cases directly from blood, samples 20 and 21 (Table 2 and Figure 3). For these samples, our NGS test detected 36% (Figure 3B) and 59% mosaicism (Figure 3C), similar to the 50% and 66% mosaicism, respectively, by an independent laboratory. Interestingly, sample 21 is from an unaffected mother whose daughter carries the exact same mutation.

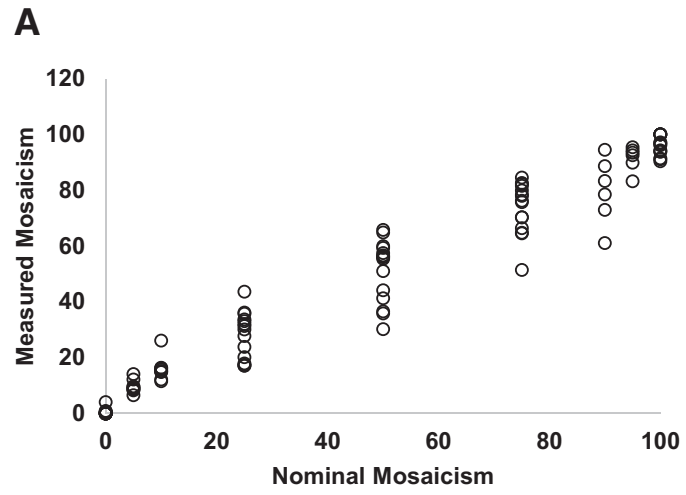

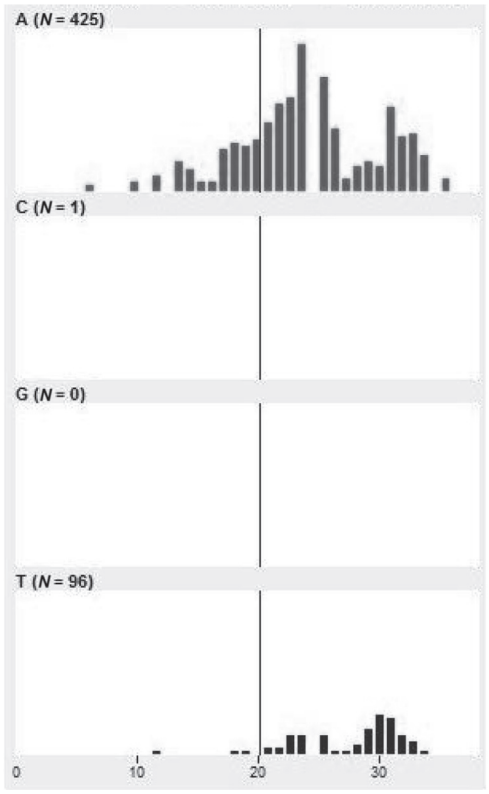

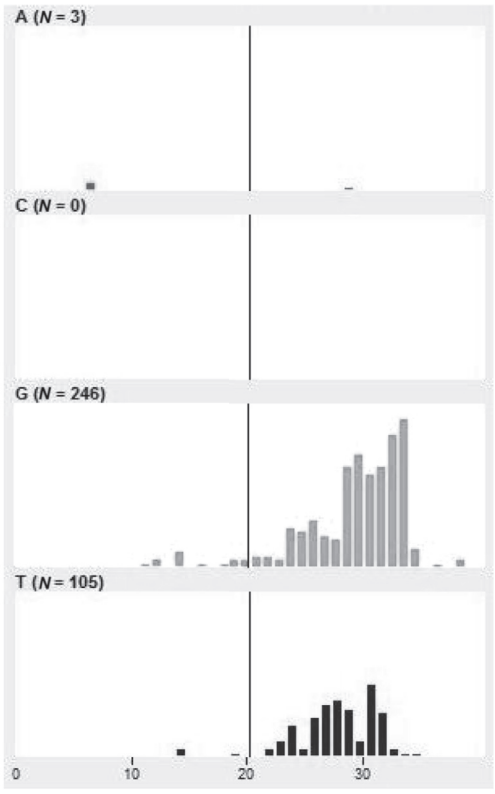

Figure 3 Evaluation of the RB1 next-generation sequencing test on mosaic mutation detection. **A:** Establishment of cutoffs for the mosaicism calling. Genomic DNA of two samples were mixed together with various proportions of each sample at 0%, 5%, 10%, 25%, 50%, 75%, 90%, 95%, and 100%, respectively. Measured mosaicism rate (*y* axis) was plotted against its nominal rate (*x* axis) on the basis of the admixture proportion of two samples. Quality scores were 10, 40, 100, 200, and 400 for <10%, 11% to 25%, 26% to 50%, 51% to 75%, and >76% of measured mosaicism, respectively. **B:** Detection of a mosaic mutation in a retinoblastoma blood sample. The frequency of the nucleotide observed at the position (*y* axis) was plotted versus Phred quality score (*x* axis). A mosaic splice mutation c.940-2A>T was detected in the retinoblastoma sample 20. **C:** Detection of a mosaic mutation in a blood sample from an unaffected relative of a retinoblastoma patient. A mosaic nonsense mutation c.508G>T (p.Glu170*) was detected in sample 21.

Promoter Mutation Detection in *RB1*

The promoter is an essential regulatory region that controls gene expression. Promoter mutations represent 1% to 2% of pathogenic mutations in *RB1*.[15,17] The *RB1* TSS was determined and validated to be located at −161 upstream from ATG using TSSer[27] and NPEST[28] algorithms, and this position is supported by at least six 5′ full-length mRNA sequences and the National Center for Biotechnology Information annotation. *RB1* has a TATA-less promoter (lacking a canonical TATA-box at −30) that also lacks the CAAT box.[31] Previous studies[31] indicate that *RB1* promoter contains binding sites for ATF and SP1 transcription factors as well as for E2F. We analyzed the *RB1* promoter sequences of isolated unilateral retinoblastoma samples with no mutation found in the *RB1* gene body, to see if we could find any

promoter mutation reported in HGMD or in the Leiden Open Variation Database (*http://rb1-lovd.d-lohmann.de/home.php?select_db=RB1*, last accessed April 2, 2014). No known pathogenic promoter mutations were found in these samples; instead, most promoter variants detected were benign SNPs found either in the 1000 Genome database (*http://www.1000genomes.org*, last accessed April 2, 2014) or in our normal reference samples. Only one promoter variant-Chr13:48875076G>T was of unknown significance. In this case, further testing of the *RB1* mRNA expression level in circulating blood and explanted tumors (where available) and in promoter reporter assays in retinoblastoma cells is needed to determine its pathogenicity. Taken together, the RB1 NGS test can be used to capture all known pathogenic mutations and, even more, it has the potential to identify novel pathogenic variants.

MYCN Copy Number Detection

MYCN copy number can also be calculated along with *RB1* copy number using Genetrix software. Blood samples from 25 retinoblastoma patients were tested for *MYCN* copy number. Because *MYCN* amplification is only reported in retinoblastoma tumors, two copies of *MYCN* were expected in blood samples. Indeed, using NGS data, *MYCN* copy number was approximately two for all 25 retinoblastoma blood samples, with an SD of 0.15 copies (Figure 4A). To confirm that the RB1 NGS test can detect *MYCN* amplification, well-characterized cell lines with known *MYCN* amplification (KCN neuroblastoma line and Y79 retinoblastoma line) were tested. *MYCN* was greatly amplified in the KCN cell line, as expected (Figure 4B). In Y79, 55 copies of *MYCN* gene were observed, higher than the published number,[32] which is probably because of different methods or further amplification of *MYCN* gene in cell culture. Because approximately 50% of retinoblastoma cases lacking detectable *RB1* gene mutations have amplification of *MYCN* with 28 to 121 copies,[26] it is important to accurately quantify *MYCN* copy number at a lower range. Different percentages of Y79 DNA ranging from 0% to 75% were spiked into normal sample NA12878, and *MYCN* copy number was measured with the RB1 NGS test. A linear relationship was observed between *MYCN* copy numbers versus the percentage of spiked-in Y79 (Figure 4C). To confirm that *MYCN* copy number measured by RB1 NGS test was correct, a similar experiment was performed using a

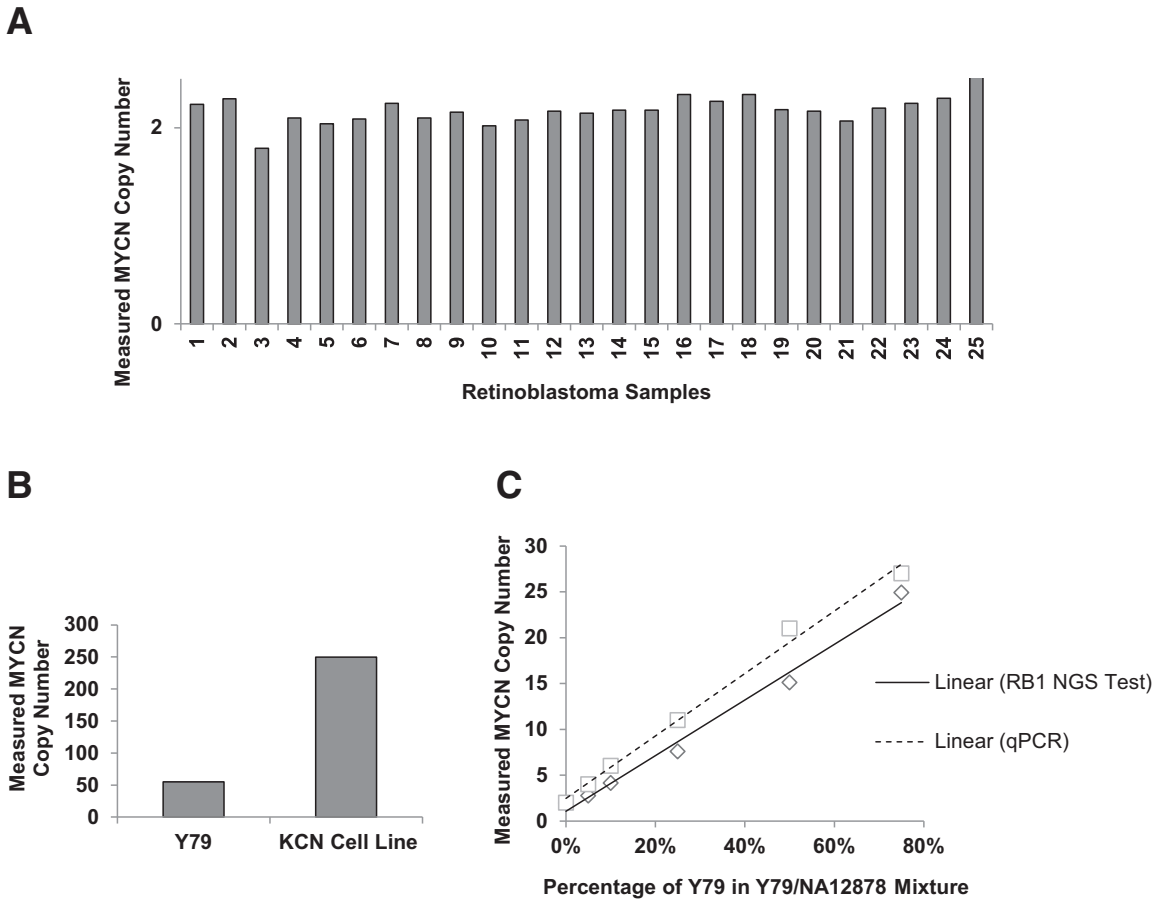

Figure 4 Quantification of MYCN copy number using the RB1 next-generation sequencing (NGS) test. **A:** *MYCN* copy number of 25 blood samples was measured with the RB1 NGS test. **B:** *MYCN* copy number of Y79 and KCN cell lines was measured. **C:** Admixture experiment was performed with different amounts of Y79 DNA spiked into normal control DNA of NA12878. The *MYCN* copy number was measured by the RB1 NGS test (solid line) as well as by the MYCN real-time quantitative PCR (qPCR) assay (broken line), and the result was plotted against the percentage of spiked-in Y79 DNA.

standard real-time quantitative PCR method, and a comparable result was obtained (Figure 4C). Because all examples of *MYCN* amplification in retinoblastoma had at least 10 *MYCN* copies, as measured by quantitative multiplex PCR or SNP analysis,[26] these data show that our NGS assay can reliably detect such changes. Therefore, the RB1 NGS test can be used to quantify *MYCN* copy number and to differentiate between normal and *MYCN* amplified retinoblastoma samples.

Discussion

Early and accurate molecular diagnosis of retinoblastoma is critical for determining the best course of treatment and appropriate surveillance measures for retinoblastoma patients. Parents and siblings can also benefit from timely testing for an *RB1* mutation found in a retinoblastoma patient. If the mutation is found in any family member, close surveillance is warranted because of the increased risk of retinoblastoma and *RB1*-associated secondary tumors, like osteosarcoma. If no germline mutation exists in the *RB1* gene, the risk of retinoblastoma in the child's contralateral eye, siblings, or other family members falls to population risk and no further surveillance is needed. So far, it has been a challenge to test the entire *RB1* gene because of its size (183 kb containing 27 exons). Historical assays have consequently focused on exonic and splice junction mutations, and have used a combination of testing methods to detect different kinds of mutations. Herein, we report an efficient and comprehensive RB1 NGS test capable of capturing various kinds of *RB1* mutations reported in the HGMD, including point mutations, small indels, large deletions/duplications, and copy number variations in the *RB1* gene on a single test platform, simplifying current *RB1* testing processes. Our test, however, could not detect *RB1* gene rearrangements, which could be potential pathogenic mutations found in retinoblastoma. In addition, this assay cannot detect *RB1* promoter hypermethylation, which is present in approximately 12% of unilateral sporadic tumors, and results in allele-specific nonexpression of *RB1* mRNA, and thus no Rb1 protein translation from that allele. When combined with inactivating mutation or deletion in the other allele, no functional Rb1 protein is present, despite the presence of a wild-type allele. However, this assay is significantly more comprehensive in its ability to detect germline defects than any prior test, and reduces overall reporting time as well as labor costs of *RB1* testing. Despite sequencing the entire *RB1* gene (approximately 183 kb), the cost of this NGS test is similar to that of currently available tests, which only sequence *RB1* exons and flanking intronic regions (approximately 2.7 kb).

A major challenge of *RB1* mutation testing is to differentiate low-level mosaic mutations from somatic RB1 mutations, which is critical for disease prognosis and genetic counseling for retinoblastoma patient families. Historically, because of the insensitivity of Sanger sequencing, low-level mosaic mutations could not be easily identified from blood samples. To capture mosaic mutations in blood, clinical laboratories have had to test the tumor first to identify the disease-causing mutation, followed by allele-specific PCR to confirm the mutation in the patient's blood and thus determine mosaicism. Because of this, some *RB1* mosaic mutations were not identified for years, until the tumor was obtained after enucleation.[33] Highly sensitive allele-specific PCR as well as an NGS-based assay have been developed previously to detect low-level mosaicism in blood samples; however, they are limited to the 11 recurrent nonsense mutations or mutations in *RB1* exons only.[14,25] The method described herein allows deep sequencing of the entire *RB1* gene, enabling us to detect mosaic mutations >5% frequency in the *RB1* promoter, untranslated regions, exons, intron/exon boundaries, and introns directly from a blood sample. With further improvements in NGS technology, including improved error rate, we expect the mosaicism detection threshold can be further reduced. This will dramatically improve the ability to detect mosaic mutations in the *RB1* gene when the mutation in the tumor is not known.

The RB1 NGS test can also be used to detect *MYCN* amplification ($MYCN^{A}$) in $RB1^{+/+}$ tumors. Usually $RB1^{+/+}/MYCN^{A}$ retinoblastoma is a large tumor with distinctive aggressive histopathology that requires immediate removal of the affected eye to achieve optimum outcomes.[26] Furthermore, RB tumors driven by *MYCN* amplification are candidates for Aurora B kinase inhibitors,[34] unlike typical RB tumors, which potentially generates a targeted treatment for $RB1^{+/+}/MYCN^{A}$ retinoblastomas. In addition, because $RB1^{+/+}/MYCN^{A}$ tumors are due to somatic amplification of the *MYCN* gene, they are not hereditary. This RB1 NGS test is the first available method that can simultaneously distinguish *RB1* mutation versus *MYCN* amplification etiology of retinoblastomas.

In summary, the NGS-based *RB1* test described herein is the first and the only test that can detect various *RB1* mutations, including point mutations, small indels, large deletions/duplications, mosaic mutations, and *MYCN* gene amplification, in a single-test platform, all within a 3-day turnaround time, at a cost no greater than current methods. This efficient, comprehensive, sensitive, rapid, and cost-effective method will enable physicians to provide better diagnosis, clinical management, and genetic counseling for retinoblastoma patients and their families.

Acknowledgments

We thank all personnel in the Department of Pathology and Laboratory Medicine at Children's Hospital Los Angeles for their kind help and support and Xiaowu Gai and Jaclyn A. Biegel for the helpful discussions on mosaic mutation detection. Initial development of the assay was at the behest of Dr. A. Linn Murphree, former Division Chief of Ophthalmology at Children's Hospital Los Angeles and codiscoverer of the *RB1* gene.

Supplemental Data

Supplemental material for this article can be found at *http://dx.doi.org/10.1016/j.jmoldx.2016.02.006*.

References

1. Lohmann DR, Gallie BL: Retinoblastoma 2000 Jul 18 [Updated 2015 Nov 19]. In GeneReviews [Internet]. Edited by Pagon RA, Adam MP, Ardinger HH, Wallace SE, Amemiya A, Bean LJH, Bird TD, Fong C, Mefford HC, Smith RJH, Stephens K. Seattle: University of Washington, 2000. Available at http://www.ncbi.nlm.nih.gov/books/NBK1452. (last revised November 19, 2015)
2. Devesa SS: The incidence of retinoblastoma. Am J Ophthalmol 1975, 80:263–265
3. Kivela T: The epidemiological challenge of the most frequent eye cancer: retinoblastoma, an issue of birth and death. Br J Ophthalmol 2009, 93:1129–1131
4. Shields CL, Shields JA: Diagnosis and management of retinoblastoma. Cancer Control 2004, 11:317–327
5. Dimaras H, Kimani K, Dimba EA, Gronsdahl P, White A, Chan HS, Gallie BL: Retinoblastoma. Lancet 2012, 379:1436–1446
6. Knudson AG Jr: Mutation and cancer: statistical study of retinoblastoma. Proc Natl Acad Sci U S A 1971, 68:820–823
7. Cavenee WK, Dryja TP, Phillips RA, Benedict WF, Godbout R, Gallie BL, Murphree AL, Strong LC, White RL: Expression of recessive alleles by chromosomal mechanisms in retinoblastoma. Nature 1983, 305:779–784
8. Friend SH, Bernards R, Rogelj S, Weinberg RA, Rapaport JM, Albert DM, Dryja TP: A human DNA segment with properties of the gene that predisposes to retinoblastoma and osteosarcoma. Nature 1986, 323:643–646
9. Fung YK, Murphree AL, T'Ang A, Qian J, Hinrichs SH, Benedict WF: Structural evidence for the authenticity of the human retinoblastoma gene. Science 1987, 236:1657–1661
10. Dunn JM, Phillips RA, Becker AJ, Gallie BL: Identification of germline and somatic mutations affecting the retinoblastoma gene. Science 1988, 241:1797–1800
11. Marees T, Moll AC, Imhof SM, de Boer MR, Ringens PJ, van Leeuwen FE: Risk of second malignancies in survivors of retinoblastoma: more than 40 years of follow-up. J Natl Cancer Inst 2008, 100: 1771–1779
12. Lohmann DR, Gerick M, Brandt B, Oelschlager U, Lorenz B, Passarge E, Horsthemke B: Constitutional RB1-gene mutations in patients with isolated unilateral retinoblastoma. Am J Hum Genet 1997, 61:282–294
13. Richter S, Vandezande K, Chen N, Zhang K, Sutherland J, Anderson J, Han L, Panton R, Branco P, Gallie B: Sensitive and efficient detection of RB1 gene mutations enhances care for families with retinoblastoma. Am J Hum Genet 2003, 72:253–269
14. Rushlow D, Piovesan B, Zhang K, Prigoda-Lee NL, Marchong MN, Clark RD, Gallie BL: Detection of mosaic RB1 mutations in families with retinoblastoma. Hum Mutat 2009, 30:842–851
15. Harbour JW: Overview of RB gene mutations in patients with retinoblastoma: implications for clinical genetic screening. Ophthalmology 1998, 105:1442–1447
16. Lohmann DR, Brandt B, Hopping W, Passarge E, Horsthemke B: The spectrum of RB1 germ-line mutations in hereditary retinoblastoma. Am J Hum Genet 1996, 58:940–949
17. Dommering CJ, Mol BM, Moll AC, Burton M, Cloos J, Dorsman JC, Meijers-Heijboer H, van der Hout AH: RB1 mutation spectrum in a comprehensive nationwide cohort of retinoblastoma patients. J Med Genet 2014, 51:366–374
18. Sonkin D, Hassan M, Murphy DJ, Tatarinova TV: Tumor suppressors status in cancer cell line Encyclopedia. Mol Oncol 2013, 7:791–798
19. Nichols KE, Houseknecht MD, Godmilow L, Bunin G, Shields C, Meadows A, Ganguly A: Sensitive multistep clinical molecular screening of 180 unrelated individuals with retinoblastoma detects 36 novel mutations in the RB1 gene. Hum Mutat 2005, 25:566–574
20. Zhang K, Nowak I, Rushlow D, Gallie BL, Lohmann DR: Patterns of missplicing caused by RB1 gene mutations in patients with retinoblastoma and association with phenotypic expression. Hum Mutat 2008, 29:475–484
21. Dehainault C, Michaux D, Pages-Berhouet S, Caux-Moncoutier V, Doz F, Desjardins L, Couturier J, Parent P, Stoppa-Lyonnet D, Gauthier-Villars M, Houdayer C: A deep intronic mutation in the RB1 gene leads to intronic sequence exonisation. Eur J Hum Genet 2007, 15:473–477
22. Brichard B, Heusterspreute M, De Potter P, Chantrain C, Vermylen C, Sibille C, Gala JL: Unilateral retinoblastoma, lack of familial history and older age does not exclude germline RB1 gene mutation. Eur J Cancer 2006, 42:65–72
23. Alonso J, Palacios I, Gamez A, Camino I, Frayle H, Menendez I, Kontic M, Garcia-Miguel P, Sastre A, Abelairas J, Sarret E, Sabado C, Navajas A, Artigas M, Indiano JM, Carbone A, Rosell J, Pestana A: Molecular diagnosis of retinoblastoma: molecular epidemiology and genetic counseling Spanish. Med Clin (Barc) 2006, 126:401–405
24. Sippel KC, Fraioli RE, Smith GD, Schalkoff ME, Sutherland J, Gallie BL, Dryja TP: Frequency of somatic and germ-line mosaicism in retinoblastoma: implications for genetic counseling. Am J Hum Genet 1998, 62:610–619
25. Chen Z, Moran K, Richards-Yutz J, Toorens E, Gerhart D, Ganguly T, Shields CL, Ganguly A: Enhanced sensitivity for detection of low-level germline mosaic RB1 mutations in sporadic retinoblastoma cases using deep semiconductor sequencing. Hum Mutat 2013, 35: 384–391
26. Rushlow DE, Mol BM, Kennett JY, Yee S, Pajovic S, Theriault BL, Prigoda-Lee NL, Spencer C, Dimaras H, Corson TW, Pang R, Massey C, Godbout R, Jiang Z, Zacksenhaus E, Paton K, Moll AC, Houdayer C, Raizis A, Halliday W, Lam WL, Boutros PC, Lohmann D, Dorsman JC, Gallie BL: Characterisation of retinoblastomas without RB1 mutations: genomic, gene expression, and clinical studies. Lancet Oncol 2013, 14:327–334
27. Troukhan M, Tatarinova T, Bouck J, Flavell RB, Alexandrov NN: Genome-wide discovery of cis-elements in promoter sequences using gene expression. OMICS 2009, 13:139–151
28. Tatarinova T, Kryshchenko A, Triska M, Hassan M, Murphy D, Neely M, Schumitzky A: NPEST: a nonparametric method and a database for transcription start site prediction. Quant Biol 2014, 1:261–271
29. Rehm HL, Bale SJ, Bayrak-Toydemir P, Berg JS, Brown KK, Deignan JL, Friez MJ, Funke BH, Hegde MR, Lyon E: ACMG clinical laboratory standards for next-generation sequencing. Genet Med 2013, 15:733–747
30. Zhao M, Wang Q, Wang Q, Jia P, Zhao Z: Computational tools for copy number variation (CNV) detection using next-generation sequencing data: features and perspectives. BMC Bioinformatics 2013, 14(Suppl 11):S1
31. Gill RM, Hamel PA, Zhe J, Zacksenhaus E, Gallie BL, Phillips RA: Characterization of the human RB1 promoter and of elements involved in transcriptional regulation. Cell Growth Differ 1994, 5: 467–474
32. Kim JH, Kim JH, Yu YS, Kim DH, Kim YK, Kim KW: Comparative genomic hybridization analysis of newly established retinoblastoma cell lines of adherent growth compared with Y79 of nonadherent growth. J Pediatr Hematol Oncol 2008, 30:571–574
33. Astudillo PP, Chan HS, Heon E, Gallie BL: Late-diagnosis retinoblastoma with germline mosaicism in an 8-year-old. J AAPOS 2014, 18:500–502
34. Hook KE, Garza SJ, Lira ME, Ching KA, Lee NV, Cao J, Yuan J, Ye J, Ozeck M, Shi ST, Zheng X, Rejto PA, Kan JL, Christensen JG, Pavlicek A: An integrated genomic approach to identify predictive biomarkers of response to the aurora kinase inhibitor PF-03814735. Mol Cancer Ther 2012, 11:710–719